Carbó, J.J., et al., 2019. A bridging bis-allyl titanium complex: mechanistic insights into the electronic structure and reactivity. Inorganic Chemistry

# A Bridging bis-Allyl Titanium Complex: Mechanistic Insights into the Electronic Structure and Reactivity

*Jorge J. Carbó,*‡ María Gómez-Pantoja,† Avelino Martín,† Miguel Mena,† Josep M. Ricart,‡ Antoni Salom-Català‡ and Cristina Santamaría*†.*

†Departamento de Química Orgánica y Química Inorgánica. Instituto de Investigación Química "Andrés M. del Río" (IQAR), Universidad de Alcalá, Campus Universitario, E-28805 Alcalá de Henares, Madrid, Spain.

‡Departament de Química Física i Inorgànica, Universitat Rovira i Virgili, Campus Sescelades, C/ Marcel.lí Domingo, s/n, 43007 Tarragona (Spain)

Supporting Information

ABSTRACT:

Treatment of the dinuclear compound [{Ti($\eta^5$-$C_5Me_5$)$Cl_2$}$_2$($\mu$-O)] with allylmagnesium chloride provides the formation of the allyltitanium(III) derivative [{Ti($\eta^5$-$C_5Me_5$)($\mu$-$C_3H_5$)}$_2$($\mu$-O)] (**1**), structurally identified by single-crystal X-ray analysis. Density functional theory (DFT) calculations confirm that the electronic structure of **1** is a singlet state, and the molecular orbital analysis, along with the short Ti-Ti distance, reveal the presence of a metal-metal single bond between the two Ti(III) centers. Complex **1** reacts rapidly with organic azides, $RN_3$ (R = Ph, $SiMe_3$), to yield the allyl $\mu$-imido derivatives [{Ti($\eta^5$-$C_5Me_5$)($CH_2CH{=}CH_2$)}$_2$($\mu$-NR)($\mu$-O)] [R = Ph(**2**), $SiMe_3$(**3**)] along with molecular nitrogen release. Reaction of **2** and **3** with $H_2$ leads to the $\mu$-imido propyl species [{Ti($\eta^5$-$C_5Me_5$)($CH_2CH_2CH_3$)}$_2$($\mu$-NR)($\mu$-O)] [R = Ph(**4**), $SiMe_3$(**5**)]. Theoretical calculations were used to gain insight into the hydrogenation mechanism of complex **3** and rationalize the lower reactivity of **2**. Initially, the $\mu$-imido bridging group in these complexes activates the $H_2$ molecule via addition to the Ti-N bonds. Subsequently, the titanium hydride intermediates induce a change in hapticity of the allyl ligands, and the nucleophilic attack of hydride to the allyl groups leads to metallacyclopropane intermediates. Finally, the proton transfer from the amido group to the metallacyclopropane moieties afford the propyl complexes **4** and **5**.

## INTRODUCTION

The first studies about transition metal allyl complexes dates to the late 1950's when Smidt and Hafner synthesized the dinuclear allyl complex $[PdCl(\eta^3\text{-}C_3H_5)]_2$ by reaction of palladium(II) chloride with allylic alcohol.[1] Since this initial report, numerous metal allyl complexes have been reported,[2] including f-block[3] and main group elements.[4] In spite of dinuclear allyl complexes were first synthesized and structurally characterized, most of the initial research focused largely on mononuclear allyl species, especially of palladium, which revealed as crucial intermediates in a wide range of organic processes.[5]

In the last years, dinuclear complexes bearing the bridging $\eta^3$-allyl moiety have attracted increasing attention because the unsaturated hydrocarbon bridging ligand prevented the cleavage to mononuclear complexes. The number of known allyl complexes comprising this chelate-bridging fragment is almost solely limited to middle-late transition metals (groups 6, 8, 9 and 10)[5c,6] with M-M bonding interaction.

Within group 4, the only crystallographically characterized $\mu$-$\eta^3$-allyl complex is the paramagnetic titanium complex, $[Ti_2(\mu\text{-}Cl)_2Cl_2(dmpe)_2(\mu\text{-}\eta^3\text{-}C_3H_5)]$, reported by Cotton and coworkers.[7] We report here the synthesis of a dinuclear bridging bis-allyl titanium complex and a detailed computational analysis of its electronic structure. In addition, we have examined the synthesis of allyl $\mu$-imido derivatives and their subsequent hydrogenation reactions both experimentally and computationally.

EXPERIMENTAL SECTION

**General Considerations**. All manipulations were carried out under a dry argon atmosphere using Schlenk-tube and cannula techniques or in a conventional argon-filled glovebox. Solvents were carefully refluxed over the appropriate drying agents and distilled prior to use: $C_6D_6$ and hexane (Na/K alloy), tetrahydrofurane (Na/benzophenone) and toluene (Na). Starting material [{Ti($\eta^5$-$C_5Me_5$)$Cl_2$}$_2$($\mu$-O)] was prepared following reported procedure.[8] Allylmagnesium chloride (2 M in thf) and $RN_3$ (R = Ph, $SiMe_3$) were purchased from Aldrich and were used without further purification. Microanalyses (C, H, N, S) were performed in a LECO CHNS-932 microanalyzer. Samples for IR spectroscopy were prepared as KBr pellets and recorded on the Perkin-Elmer IR-FT Frontier spectrophotometer (4000-400 $cm^{-1}$). $^1H$ and $^{13}C$ NMR spectra were obtained by using Varian NMR System spectrometers: Unity-300 Plus, Mercury-VX and Unity-500, and reported with reference to solvent resonances. $^1H$-$^{13}C$ gHSQC were recorded using the Unity-500 MHz NMR spectrometer operating at 25 °C.

**Synthesis of [Ti$_2$($\eta^5$-C$_5$Me$_5$)$_2$($\mu$-CH$_2$CHCH$_2$)$_2$($\mu$-O)] (1).** A 100 mL J-Young Carious tube was charged with [{Ti($\eta^5$-$C_5Me_5$)$Cl_2$}$_2$($\mu$-O)] (1.00 g, 1.91 mmol) and filled up with 50 mL of thf. The resulting orange solution was cooled to -78 °C. A solution of 4 mL (8 mmol) of allylmagnesium chloride in 10 mL of thf was added to the reaction solution. The reaction mixture was stirred and warmed at room temperature for 2 h, and slowly the color changed from orange to dark blue. The solvent was removed under reduced pressure and the solid was extracted with hexane. The filtrated was concentrated to half volume and cooled at -20 °C to give dark blue crystals identified as **1** (Yield: 0.81 g, 91%). IR (KBr, $cm^{-1}$): $\bar{\nu}$ = 2963 (m), 2939 (m), 2902 (s), 2653 (m), 1492 (w), 1432 (m), 1375 (m), 1262 (m), 1206 (m), 1097 (m), 1023 (m), 944 (m), 786 (vs), 634 (s), 615 (s). $^1H$ NMR ($C_6D_6$, 500 MHz, 298 K): $\delta$ = 1.05, 1.67 (overlap.) ($A_2M_2X$ syst. bs, 8H, C$H_2$CHC$H_2$), 1.67 (s, 30 H, $C_5Me_5$), 6.16 ($A_2M_2X$ syst., 2H, $CH_2CHCH_2$). $^{13}C\{^1H\}$ NMR ($C_6D_6$, 125 MHz, 298 K): $\delta$ = 10.9 ($C_5Me_5$), 72.8 ($CH_2CHCH_2$), 109.9 ($CH_2CHCH_2$), 116.0 ($C_5Me_5$). Elemental analysis (%) calcd. for $C_{26}H_{40}OTi_2$ (464.33): C, 67.25; H, 8.68; found: C, 66.86; H, 8.03.

**Preparation of [Ti$_2$($\eta^5$-C$_5$Me$_5$)$_2$(C$_3$H$_5$)$_2$($\mu$-NPh)($\mu$-O)] (2).** To a solution of **1** (0.40 g, 0.86 mmol) in hexane (50 mL) was added 175 $\mu$L (0.86 mmol) of $PhN_3$. After stirring for 30 minutes, the reaction

mixture was filtered, and the solvent was removed under reduced pressure to give an orange crystalline foam (0.35 g, 73%) identified as **2**. IR (KBr, $cm^{-1}$): $\bar{\nu}$ = 2909 (s), 1601 (m), 1583 (w), 1498 (w), 1476 (m), 1431 (w), 1376 (m), 1262 (s), 1023 (m), 786 (vs), 659 (s), 525 (m). $^1$H NMR ($C_6D_6$, 500 MHz, 298 K): $\delta$ = 1.85 (s, 30H, $C_5Me_5$), 3.81 ($A_4X$ syst., 8H, $J$ = 11 Hz, $CH_2CHCH_2$), 6.53 ($A_4X$ syst., 2H, $J$ = 11 Hz, $CH_2CHCH_2$), 6.2-7.5 (m, 5H, N*Ph*). $^{13}$C{$^1$H} NMR ($C_6D_6$, 125 MHz, 298 K): $\delta$ = 11.5 ($C_5Me_5$), 85.0 ($CH_2CHCH_2$), 122.9 ($C_5Me_5$), 121.5, 122.8, 128.4. 156.2 (N*Ph*), 143.4 ($CH_2CHCH_2$). MS (EI, 70 eV), *m/z* (%): 514 (100) $[M-C_3H_5]^+$, 473 (52) $[M-2C_3H_5]^+$. We were unable to obtain satisfactory elemental analysis for this complex.

**Preparation of $[Ti_2(\eta^5\text{-}C_5Me_5)_2(C_3H_5)_2(\mu\text{-}NSiMe_3)(\mu\text{-}O)]$ (3).** In a similar fashion to complex **2**, the reaction between **1** (0.50 g, 1.08 mmol) and $Me_3SiN_3$ (138 $\mu$L, 0.118 g, 1.08 mmol) in 50 mL of hexane gives compound **3** as an orange reddish solid in good yield (0.54 g, 91%). The $^1$H NMR revealed the presence of a mixture of two isomers in ca. 1:3 ratio. IR (KBr, $cm^{-1}$): $\bar{\nu}$ = 2955 (m), 2910 (s), 1603 (s), 1494 (w), 1434 (m), 1377 (m), 1246 (s), 1177 (m), 1022 (m), 920 (vs), 831 (s), 754 (s), 661 (s), 607 (m). $^1$H NMR ($C_6D_6$, 500 MHz, 298 K): Major isomer: $\delta$ = 0.03 (s, 9H, NSi$Me_3$), 1.97 (s, 30H, $C_5Me_5$), 3.95 ($A_4X$ syst., 8H, $J$ = 11 Hz, $CH_2CHCH_2$), 6.58 ($A_4X$ syst., 2H, $J$ = 11 Hz, $CH_2CHCH_2$). Minor isomer: $\delta$ = 0.13 (s, 9H, NSi$Me_3$), 1.99 (s, 30H, $C_5Me_5$), 3.69 ($A_4X$ syst., 8H, $J$ = 11 Hz, $CH_2CHCH_2$), 6.33 ($A_4X$ syst., 2H, $J$ = 11 Hz, $CH_2CHCH_2$). $^{13}$C{$^1$H} NMR ($C_6D_6$, 125 MHz, 298 K): Major isomer: $\delta$ = 5.0 (NSi$Me_3$), 12.1 ($C_5Me_5$), 84.8 ($CH_2CHCH_2$), 122.5 ($C_5Me_5$), 144.9 ($CH_2CHCH_2$). Minor isomer: $\delta$ = 5.4 (NSi$Me_3$), 12.5 ($C_5Me_5$), 87.8 ($CH_2CHCH_2$), 122.2 ($C_5Me_5$), 143.6 ($CH_2CHCH_2$). Elemental analysis (%) calcd. for $C_{29}H_{49}NOSiTi_2$ (551.52): C, 63.15; H, 8.95; N, 2.54; found: C, 62.94; H, 8.38; N, 3.37.

**Reaction of $[Ti_2(\eta^5\text{-}C_5Me_5)_2(C_3H_7)_2(\mu\text{-}NPh)(\mu\text{-}O)]$ (4).** A J-Young NMR tube was charged with 20 mg (0.036 mmol) of **2** dissolved in ca. 1.0 mL of $C_6D_6$. The solution was subsequently placed under 1.5 atm $H_2$ gas, and was left at room temperature for a week to give **4** as unique product. This complex was characterized by NMR spectroscopy *in situ* without isolation. $^1$H NMR ($C_6D_6$, 500 MHz, 298 K): $\delta$ = 0.75-2.50 ($CH_2CH_2CH_3$), 1.87 (s, 30H, $C_5Me_5$), 6.21-7.10 (m, 5H, N*Ph*). $^{13}$C{$^1$H} NMR ($C_6D_6$, 125 MHz, 298 K): $\delta$ = 11.2 ($C_5Me_5$), 21.4 ($CH_2CHCH_3$), 25.3 ($CH_2CH_2CH_3$), 63.7 ($CH_2CH_2CH_3$), 121.7 ($C_5Me_5$), 122.0-155.9 (N*Ph*).

**Preparation of [$Ti_2(\eta^5$-$C_5Me_5)_2(C_3H_7)_2(\mu$-$NSiMe_3)(\mu$-O)] (5).** A 100 mL Carius tube was charged with **3** (0.50 g, 0.91 mmol) and 25 mL of hexane. The solution was subsequently placed under 1.5 atm $H_2$ gas, and was left stirring at room temperature for two days. After that, the Carius tube was opened in a glove-box, the solution was filtered and then the solvent was removed in vacuum to yield a yellow greenish solid identified as **5** (0.48 g, 95%). The $^1$H NMR revealed the presence of a mixture of two isomers in a 1:5 ratio. IR (KBr, cm$^{-1}$): $\bar{\nu}$ = 2950 (s), 2913 (s), 2859 (s), 1495 (w), 1447 (m), 1376 (s), 1024 (m), 926 (vs), 832 (vs), 753 (s), 660 (vs), 611 (m). $^1$H NMR ($C_6D_6$, 500 MHz, 298 K): Major isomer: $\delta$ = 0.12 (s, 9H, NSi*Me*$_3$), 1.17 (t, 6H, *J* = 7 Hz, $CH_2CH_2CH_3$), 1.46 (m, 4H, *J* = 12 Hz, $CH_2CH_2CH_3$), 1.74 (m, 4H, *J* = 7, 12 Hz, $CH_2CH_2CH_3$), 2.01 (s, 30H, $C_5Me_5$). Minor isomer: $\delta$ = 0.05 (s, 9H, NSi*Me*$_3$), 1.22 (t, 6H, *J* = 7 Hz, $CH_2CH_2CH_3$), 1.25-1.80 ($CH_2CH_2CH_3$), 1.98 (s, 30H, $C_5Me_5$). $^{13}$C{$^1$H} NMR ($C_6D_6$, 125 MHz, 298 K): Major isomer: $\delta$ = 5.4 (NSi*Me*$_3$), 12.0 ($C_5Me_5$), 21.3 ($CH_2CHCH_3$), 25.8 ($CH_2CH_2CH_3$), 64.5 ($CH_2CH_2CH_3$), 121.4 ($C_5Me_5$). Minor isomer: $\delta$ = 4.9 (NSi*Me*$_3$), 12.3 ($C_5Me_5$), 21.5 ($CH_2CH_2CH_3$), 26.9 ($CH_2CH_2CH_3$), 70.0 ($CH_2CH_2CH_3$), 121.0 ($C_5Me_5$). Elemental analysis (%) calcd. for $C_{29}H_{53}NOSiTi_2$ (555.55): C, 62.70; H, 9.62; N, 2.52; found: C, 62.97; H, 9.98; N, 3.26.

**Crystal structure determination of complexes 1, 2 and 5**. Crystals of **1**, **2** and **5** were obtained by slow cooling at -20 °C of the corresponding hexane solutions. Single crystals were coated with mineral oil, mounted on Mitegen MicroMounts with the aid of a microscope, and immediately placed in the low temperature nitrogen stream of the diffractometer. The intensity data sets were collected at 200 K on a Bruker-Nonius KappaCCD diffractometer equipped with graphite-monochromated Mo Kα radiation (λ = 0.71073 Å) and an Oxford Cryostream 700 unit. Crystallographic data for all complexes are presented in Table S1 in the Supporting Information.

The structures were solved, by using the WINGX package,[9] by direct methods (SHELXS-2013)[10] and refined by least-squares against F2 (SHELXL-2014).[9] Compound **5** crystallized with two crystallographically independent molecules. All non-hydrogen atoms were anisotropically refined, while hydrogen atoms were placed at idealized positions and refined using a riding model, except hydrogen atoms of the allyl ligands in complex **1**, that were located in the difference Fourier map and isotropically refined. Molecules of **2** presented disorder in the terminal carbon atoms of the allyl ligands

(C43 and C53); two sites were found for each carbon atom with optimized occupancies of 64% and 36% respectively. C31-C36 of the phenyl ring in **2** were slightly disordered and EADP[9] restraints were applied to obtain a sensible chemical model.

**Computational Details**. Calculations were performed with Gaussian16 program package[11] within the framework of the density functional theory (DFT)[12] using the B3LYP functional[13] for the general study. The basis set for titanium and silicon atoms was associated with a pseudopotential,[14] with a standard double-ξ LANL2DZ contraction, and the basis set was supplemented by f and d shells, respectively.[15] The rest of atoms were described with a standard 6-31G (d, p) basis set.[16] The stationary points were located without any restriction. Transition states were characterized by a single imaginary frequency, whose normal mode corresponded to the expected motion. We also applied a GD3 dispersion correction[17] and a correction on ΔG values of 1.89 kcal·mol$^{-1}$ to change the reference state from the ideal gas standard state of 1 atm (0.041 mol·L$^{-1}$) to 1 mol·L$^{-1}$ in liquid solution (see Supporting Information for further details). The natural bond orbital (NBO) method was used to compute atomic charges.[18]

## RESULTS AND DISCUSSION

The reaction of the $\mu$-oxo tetrachloro dititanium complex [{Ti($\eta^5$-$C_5Me_5$)$Cl_2$}$_2$($\mu$-O)][8] with 4 equivalents or excess of allylmagnesium chloride in hexane at -78 ºC for 2 h afforded the bis-allyl derivative [{Ti($\eta^5$-$C_5Me_5$)($\mu$-$C_3H_5$)}$_2$($\mu$-O)] (**1**) in high yields (> 90 %) (Scheme 1). This reaction is accompanied by a dramatic change color from bright orange to dark blue. Compound **1** is quite soluble in common solvents such as benzene, toluene or tetrahydrofuran, and scarcely soluble in hexane, and it should be stored at low temperature under inert conditions to prevent its decomposition in solution. Fortunately, its nature could be determined by a single crystal X-ray diffraction analysis.

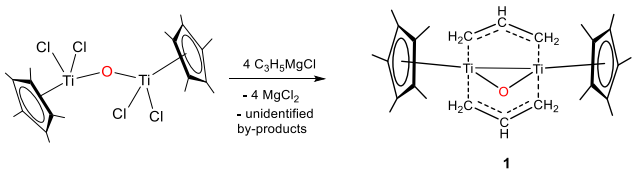


**Scheme 1.** Synthesis of the $\mu$-allyl titanium complex **1**.

Crystal structure of **1** is shown in Figure 1 and consists of a dinuclear species comprising two Ti($\eta^5$-$C_5Me_5$) units bridged by one oxygen atom and two allyl ligands, where the geometry around both titanium atoms is close to a three-legged piano stool arrangement. The allyl groups and the oxo bridge optimize the available space and, therefore, the two pentamethylcyclopentadienyl rings form angles of ~60° with the plane defined by O1, C32 and C42.

The most remarkable feature of **1** is the presence of the two bridging allyl groups. The allyl bridges are highly symmetrical with C31, C33, C41 and C43 being almost equidistant to Ti1 and Ti2 (Ti–C$_\alpha$, 2.165(3)-2.191(3) Å). These distances are longer than those found in Ti(IV) derivatives comprising three bridging ligands, such as [$Ti_2$($\eta^5$-$C_5Me_5$)$_2$($\mu$-$CH_2SiMe_2CH_2$)$_2$($\mu$-O)] (Ti-C = 2.104(9)Å),[19] but quite similar to that found in Cotton's (2.154(6) Å).[7] Additionally, the central carbon atoms, C32 and C42, are significantly farther but equidistant from the two titanium atoms with distances (av. 2.636(9) Å) significantly longer than that found in Cotton's (2.430(6) Å). The C–C–C angle of ≈125° in the allyl group is quite normal. There is a little increase in carbon–carbon bond distances within the allyl ligand upon coordination (av. 1.416(2) Å), although still in the same range that values found in mononuclear,

[TiCl(depe)($\eta^3$-$C_3H_5$)$_2$] (C-C = 1.362(4)-1.397(4) Å)[7] and [Ti($\eta^5$-$C_5H_5$)($\eta^5$-$C_5Me_5$)($\eta^3$-allyl)] (C-C = 1.38(1) Å),[20] or dinuclear with two bridged allyl ligands, [Ti$_2$($\mu$-Cl)$_2$Cl$_2$(dpme)$_2$($\mu$-$\eta^3$-$C_3H_5$)] (C-C= 1.433(1) Å),[7] and [W$_2$($\mu$-$C_3H_5$)$_2$(NMe$_2$)$_4$] (C-C = 1.47(1) Å)[21] derivatives.

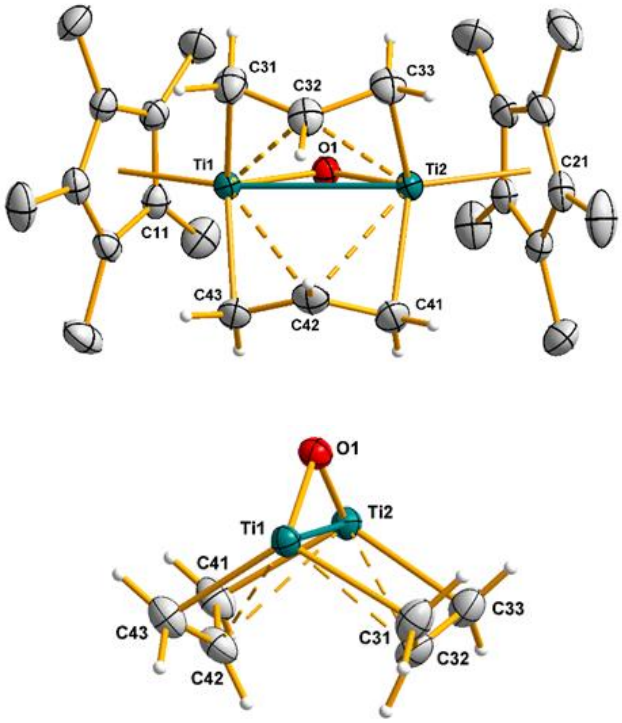


**Figure 1**. Molecular structure of **1** (top) and simplified view of the core (bottom).

Additionally, the central carbon atoms of the bridging allyl ligands are canted toward the Ti centers. As a result, the dihedral angle between each bridging allyl plane and the plane containing the two Ti atoms and the two terminal carbon atoms of the bridging allyl ligand is ~84°. Finally, the existence of the three bridging groups shortens significantly the distance Ti1···Ti2 (2.905(1) Å) in comparison with the starting complex [{Ti($\eta^5$-$C_5Me_5$)Cl$_2$}$_2$($\mu$-O)] (3.604 Å) and other dinuclear Ti(IV) compounds,[19] but comparable to that found in Cotton's (2.908(1) Å). Accordingly, we can observe that the narrow Ti1-O-Ti2 angle (104.4(1)°) is comparable to other known titanium dinuclear $\mu$-oxo compounds with additional bridge ligands.[19] The Ti-O bond lengths (av. 1.838(1) Å) are in the same range of values found for other di-, tri- or tetranuclear titanium species.[8,22]

The $^1$H and $^{13}$C NMR spectra of compound **1** revealed a diamagnetic behavior in solution, in contrast to the paramagnetism found in Cotton's derivative. These spectra show the equivalence of the $\eta^5$-$C_5Me_5$ ligands, with only one signal in the $^1$H NMR spectrum ($\delta$ = 1.67) and two in the $^{13}$C{$^1$H} NMR spectrum

($\delta$ = 10.9 $C_5Me_5$; 116.0 $C_5Me_5$), significantly shifted of the usual region for high valent dinuclear pentamethylcyclopentadienyl $\mu$-oxo titanium complexes.[19,23] The allyl ligand displays a broad doublet centered at $\delta$ 1.05 for the *anti*/*syn* protons. A peak found at $\delta$ 1.67 was assigned to the *anti*/*syn* proton of the allyl group, but it is overlapped by the resonance for the ring methyl protons. In the $^{13}C$ NMR spectrum the terminal allylic carbons were located at $\delta$ 72.8 and the resonance at $\delta$ 109.9 was assigned to the internal allylic carbons.

To elucidate the electronic structure and the nature of bonding in complex **1** between the allyl bridging ligands and the two titanium centers, we performed a DFT study. Using the X-ray structure as starting point, geometry optimizations were performed for two spin states: singlet and triplet. The different structures are shown in Figure 2, and in order to compare experimental and calculated structures some important geometric parameters are shown in Table 1.

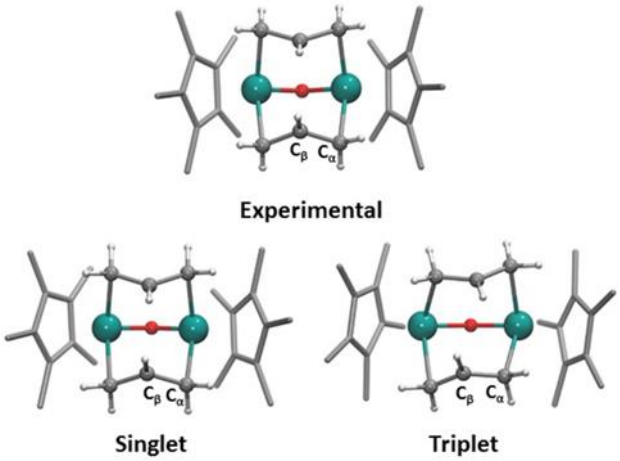


**Figure 2**. Comparison of X-ray and computed molecular structures at different spin states for **1**.

**Table 1.** Selected geometrical parameters of experimental and calculated structures for two spin states (singlet and triplet) of complex **1**. Distances in Å and angles in deg.

| | Experimental | Singlet | Triplet |
|---|---|---|---|
| Ti-Ti | 2.905(1) | 2.881 | 3.219 |
| Ti-$C_\alpha$ | 2.165(3)-2.191(3) Å) | 2.168 | 2.338 |
| Ti-$C_\beta$ | 2.636(9) | 2.626 | 2.947 |
| Ti-O-Ti | 104.4(1) | 104 | 125 |

The DFT calculations reveal that the singlet structure is favored respect the triplet one by 6.2 kcal·mol$^{-1}$, in agreement with the diamagnetic behavior observed in solution for complex **1**.

Furthermore, the geometrical features are in good agreement with those of X-ray. To gain further information about the electronic structure, we performed a molecular orbitals analysis of complex **1** at the singlet spin state ($^1$**1**). The Highest Occupied Molecular Orbital (HOMO) and Lowest Unoccupied Molecular Orbital (LUMO), are shown in Figure 3. The HOMO consists of bonding combination of atomic d-type orbitals centered at both titanium centers, which is a clear indication of $\sigma$ Ti-Ti bonding between two Ti(III) centers. The LUMO is a non-bonding molecular orbital formed by two $d_{z2}$–type atomic orbitals centered at both titaniums. The very large energy gap between the HOMO and LUMO, ~3 eV, further supports the experimental diamagnetic behavior.

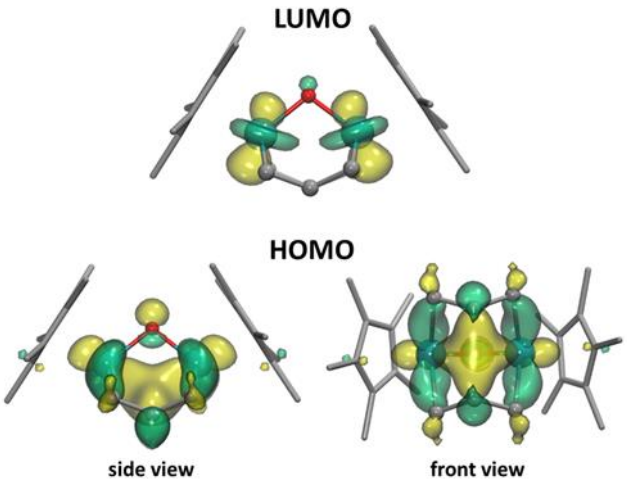


**Figure 3**. Frontier Molecular Orbitals of singlet state of complex **1**.

In an attempt to investigate the chemical behavior of the allyl complex **1**, we decided to displace the bridging allyl ligands preserving the nuclearity of complex **1**. Addition of equimolecular amounts of commercially available azides $RN_3$ (R = Ph, $SiMe_3$) to a hexane solution of **1** rendered the allyl $\mu$-imido complexes [Ti($\eta^5$-$C_5Me_5$)($CH_2CH{=}CH_2$)]$_2$($\mu$-NR)($\mu$-O) [R = Ph(**2**), $SiMe_3$(**3**)] and liberated molecular nitrogen, according to Scheme 2. The confirmation of their molecular structures came from the X-ray diffraction analysis for compound **2**.

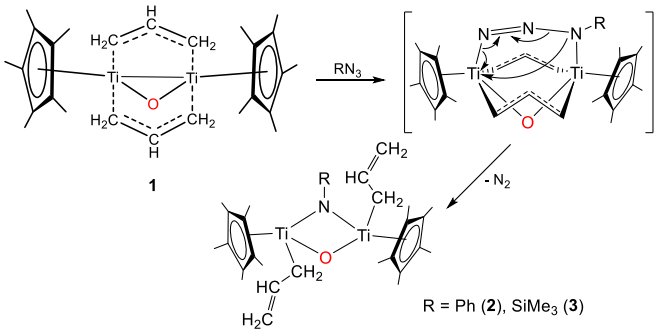


**Scheme 2**. Reactions of **1** with azides, $RN_3$ (R = Ph, $SiMe_3$).

In the formation of the $\mu$-imido complexes **2** and **3**, a possible pathway is considered in Scheme 2. Initially, the reaction would begin with the coordination of the azide to both metal centers prior to dinitrogen extrusion. It is known the zwitterionic character of the linear $RN_\alpha N_\beta N_\gamma$ moiety (Figure 4), where the major basicity on the $N_\alpha$ (form **B**) and $N_\gamma$ (form **A**), suggests the most likely binding sites for coordination to the titanium centers. Subsequently, the triazaoxodimetallacycle intermediate would proceed by loss of dinitrogen to give the $\mu$-imido complexes **2** and **3**. The formation of an analogous intermediate was tentatively proposed in the literature for other dinuclear compounds.[24]

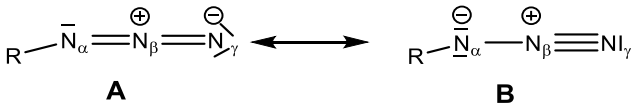


**Figure 4**. Resonance forms of organic azides.

Upon slow cooling at -20 °C for several days, single crystals of **2** precipitated from a saturated hexane solution. The molecular structure is shown in Figure 5 and selected data are listed in Table 2. Complex **2** consists of two [Ti($\eta^5$-$C_5Me_5$)$C_3H_5$] units bridged by an oxygen atom and an imido moiety, in which the pentamethylcyclopentadienyl rings are placed in the *trans*-position relative to the [$Ti_2NO$] core. The geometry around each titanium atom corresponds to the common three-legged piano stool arrangement. The Ti-O bond lengths of av. 1.853(2) Å are in the range found for other di-, tri- or tetranuclear oxotitanium species.[8,19,22,23] Additionally, the Ti-N bonds of av. 1.89(3) Å are slightly shorter than those found for the titanium $\mu$-imido $\mu$-oxo complex, [{Ti($\eta^5$-$C_5Me_5$)($\mu$-O)}$_3$(CH=CHPh)($\mu$-NPh)] (1.957(6)-1.948(6) Å),[25] but close to those reported for dinuclear titanium $\mu$-imido compounds such as [Ti($\eta^5$-$C_5H_5$)($CH_2SiMe_3$)($\mu$-NAr)]$_2$ (Ar = 3,5-$Me_2C_6H_3$) (av. 1.86-2.07 Å)[26] and [{(Ti($\eta^5$-$C_5Me_5$)Cl)($\mu$-N(4-$ClC_6H_4$))}$_2$] (1.911(2) Å).[27] The Ti-$C_\alpha$ (av. 2.16(2) Å) bond lengths are in the expected range for a

Ti(IV)-C($sp^3$)[28] bond, and the distances $C_\beta$-$C_\gamma$ (av. 1.32(8) Å) are assignable to carbon-carbon double bonds. The presence of the $\mu$-imido fragment shortens significantly the distance Ti1···Ti2 (2.782(2) Å), in comparison with **1** (2.905(1) Å) or another related compounds.[25,26,27]

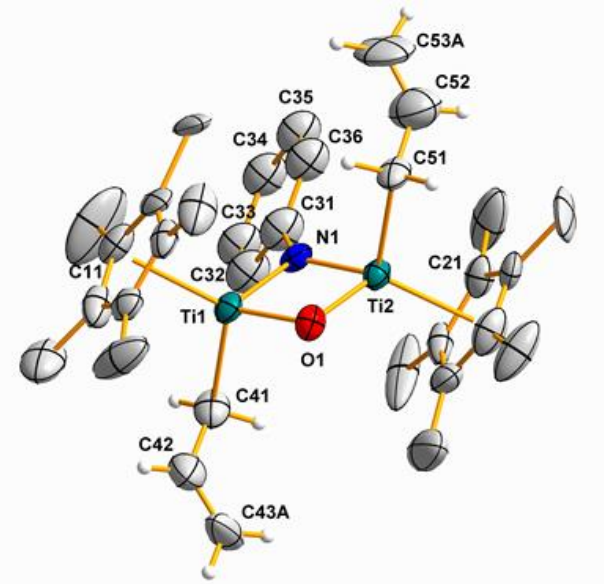


**Figure 5**. Molecular structure of complex **2** with 40% thermal ellipsoids.

**Table 2**. Selected averaged lengths (Å) and angles (°) for compounds **1**, **2** and **5**.

| Complexes | **1** | **2** | **5** |
|---|---|---|---|
| Ti···Ti | 2.905(1) | 2.782(2) | 2.759(3) |
| Ti-$C_\alpha$ | 2.18(1) | 2.16(2) | 2.129(3) |
| $C_\alpha$-$C_\beta$ | 1.417(2) | 1.46(3) | 1.515(5) |
| $C_\beta$-$C_\gamma$ | 1.419(1) | 1.32(8) | 1.520(5) |
| Ti-O-Ti | 104.4(1) | 97.3(5) | 98.2(1) |
| Ti-N-Ti | --- | 94.5(5) | 90.4(1) |

The titanium imido complexes **2** and **3** display $^1$H and $^{13}$C NMR spectra consistent with symmetrical structures, with one binary axis passing through the bridging oxygen and nitrogen atoms. Moreover, complex **3** exists as a mixture of isomers as revealed by its NMR spectra. Thus, the spectra show the equivalence of the $\eta^5$-$C_5Me_5$ ligands, with only one signal in the $^1$H NMR spectra [$\delta$ = 1.85 (**2**), 1.97/1.99 (**3**)] and two in the $^{13}C\{^1H\}$ NMR spectra [$\delta$ = 11.5 (**2**), 12.1/12.5 (**3**) $C_5Me_5$; 122.9 (**2**), 122.5/122.2 (**3**) $C_5Me_5$). The allyl resonances exhibit the well-known $\eta^1$-$\eta^3$ isomerization on the NMR timescale at room temperature, and the equivalence of the all methylene protons is observed [$\delta$ 3.81 ($J$ = 11 Hz) (**2**), $\delta$ 3.95/3.69 ($J$ = 11 Hz) (**3**)], as result of an $A_4X$ coupling pattern. The chemical shifts of the methine protons are recorded at $\delta$ 6.53 ($J$ = 11 Hz) (**2**) and $\delta$ 6.58/6.33 ($J$ = 11 Hz) (**3**). The resonances for the

methine and methylene carbons appear at $\delta$85.0 and 143.4 (**2**) and $\delta$84.8/87.8 and 144.9/143.6 ppm (**3**) respectively. The low-temperature $^1$H NMR spectra of **3** performed between room temperature and -90 °C does not show the split of the doublet; only a progressive broadening of the methylene protons signal that practically disappears into the base line, whereas the methine proton resonance remains sharp (see Figure S9). Additionally, the IR spectra (KBr pellets) show moderate absorptions at 1603 (**2**) and 1601 (**3**) cm$^{-1}$ that can be assigned to the asymmetric stretching vibration of $\eta^1$-allyl ligands,[4] in agreement with the single-crystal X-ray diffraction analysis for compound **2**.

We have evaluated computationally the possible structural isomers for complexes **2** and **3**, in which the pentamethylcyclopentadienyl rings can be placed in the *trans*- or *cis*-position relative to the [$Ti_2NO$] core, in a similar manner to those found for the dinuclear tantalum complexes, [$Ta_2(\eta^5$-$C_5Me_5)_2R_2(\mu$-$S)_2$] ( R = Me, $CH_2Me$), previously published in our research group[29]. Figure 6 shows the molecular structures of the two possible isomers for each complex and their relative free energies. For complex **2**, in which the substituent of imido moiety is a phenyl group, the *trans*-isomer is clearly favored respect to the *cis* one by 4.0 kcal·mol$^{-1}$, in agreement with the experimental observation of a single isomer. In **2**-*cis* isomer, we identified a repulsive steric interaction between the two $\eta^5$-$C_5Me_5$ ligands, while in **2**-*trans* isomer, the two rings are apart to each other and a weak stabilizing interaction between the aromatic phenyl rings and the C-H bonds of the methyl groups can take place. Replacing the phenyl substituent of the imido ligand by a hydrogen, we switch off the stabilizing C-H···phenyl interaction and the energy difference between the two isomers reduces from 4.0 to 1.7 kcal·mol$^{-1}$. This means that the destabilization of isomer **2**-*cis* by 4 kcal·mol$^{-1}$ can be attributed to the loss of two weak C-H···phenyl interactions (-1.1 kcal·mol$^{-1}$ each) and to the steric repulsion between $\eta^5$-$C_5Me_5$ units (-1.7 kcal·mol$^{-1}$). On the other hand, the repulsive interaction between the $\eta^5$-$C_5Me_5$ ligands in **3**-*cis* isomer is compensated by the repulsive interaction of trimethylsilyl substituent of the imido group with the $\eta^5$-$C_5Me_5$ ligands in **3**-*trans* (see Figure 6), resulting in two isoenergetic structures that can be found experimentally. Accordingly, the replacement of $SiMe_3$ by model $SiH_3$ substituent breaks the degeneracy favoring the *trans*-isomer by 2.2 kcal·mol$^{-1}$.

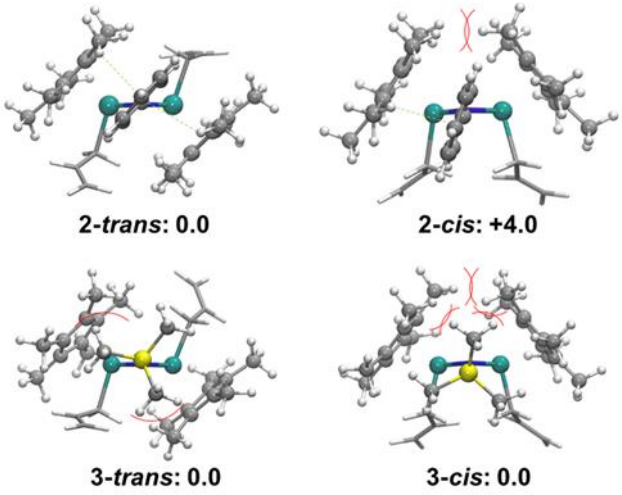


**Figure 6**. DFT structures of the *trans*- and *cis*-isomers of complexes **2** and **3**. Relative free-energies in kcal·mol$^{-1}$.

Reactivity of complexes **2** and **3** was examined by exposure of these species to $H_2$, and while no reaction was observed in case of complex **2** at p < 1 atm, compound **3** undergoes the corresponding hydrogenation process of the allyl fragments. Upon monitoring the reaction of complex **3** with dihydrogen (p < 1 atm) in an NMR tube in benzene-$d_6$ at room temperature, the presence of the $\mu$-imido propyl derivative [{Ti($\eta^5$-$C_5Me_5$)($CH_2CH_2CH_3$)}$_2$($\mu$-$NSiMe_3$)($\mu$-O)] (**5**), as a unique reaction product, was identified. A yellow greenish crystalline solid is obtained in 95% yield upon workup (Scheme 3). However, when the reactions took place at p ≈ 1.5 atm $H_2$ gas, a significant decrease of the reaction time was observed in case of **3** (two days), while complex **2** reacts cleanly to provide the corresponding $\mu$-imido propyl derivative **4** after one week at room temperature (Scheme 3).

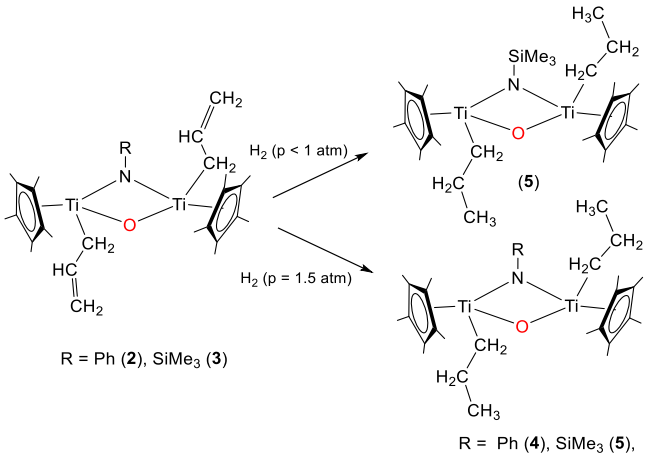


**Scheme 3**. Hydrogenation processes of complexes **2** and **3**.

Crystals of complex **5** proved to be useful for an X-ray structure analysis and revealed the structure depicted in Scheme 3. The solid-state structure is shown in Figure 7, and a selection of interatomic distances and angles data are listed in Table 2. Complex **5** shows some structural analogies with compound **2** and, therefore, it comprises a dinuclear species where the titanium atoms adopt a three-legged piano stool arrangement with a $\mu$-imido fragment, an alkyl group and an oxygen atom occupying the base positions and the $C_5Me_5$ ring in the apical vertex. Distances and angles around each titanium center are like those found in complex **2**. As distinctive feature in compound **5**, the bond distances $C_\beta$-$C_\gamma$ (av. 1.520(5) Å) of the alkyl ligands are typical of carbon-carbon single bonds, as result of the hydrogenation process on the allyl fragments.

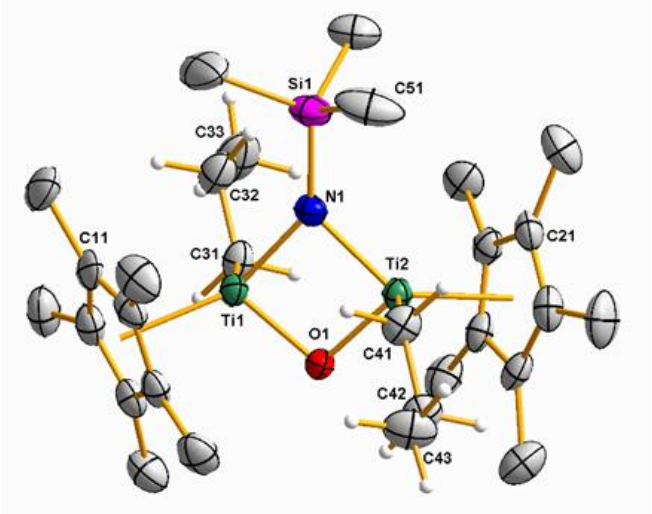


**Figure 7**. Molecular structures of complex **5** with 50% thermal ellipsoids.

Complexes **4** and **5** display a symmetrical structure in solution by NMR spectroscopy, in a similar fashion to compounds **2** and **3** respectively. As remarkable feature, the spectra of **5** revealed the presence of two isomers (see Experimental Section for the minor isomer of **5**). The NMR spectra of **4** and **5** show the equivalence of the $\eta^5$-$C_5Me_5$ ligands, with only one signal in the $^1$H NMR spectra at $\delta$ = 1.87 (**4**), 2.01 (**5**) and two in the $^{13}C\{^1H\}$ NMR spectra at $\delta$ 11.2 (**4**), 12.0 (**5**) ($C_5\mathit{Me}_5$) and $\delta$ 121.7 (**4**), 121.4 (**5**) ($\mathit{C}_5Me_5$). Distinguishing features of **4** and **5** are the resonances for the propyl ligands between $\delta$ 0.75-2.50 (**4**) and 1.10-1.80 ppm (**5**) in the $^1$H NMR spectra, and the three signals at 21.4 (**4**)/21.3 (**5**), 25.3 (**4**)/25.8 (**5**) and 63.7 (**4**)/64.5 (**5**) ppm in the $^{13}C\{^1H\}$ NMR, that evidence the hydrogenation process of the $\mu$-allyl fragments.

To understand the observed hydrogenation processes and the differences in reactivity between complexes **2** and **3**, we performed a detailed DFT study on the reaction mechanism. We focused on the hydrogenation of one of the allyl fragments, assuming that the hydrogenation at the other one proceeds in a similar way. Figure 8 shows the Gibbs free energy profile (see Supporting information for more details) of the full mechanism for the reactive complex **3** (R = $SiMe_3$) and the first hypothetic step of the less-reactive compound **2** (R = Ph). Figure 9 collects the structures and main geometric parameters of key intermediates and transition states of complex **3**.

Initially, we evaluated the energy cost associated with the direct hydrogenation of the double bond in a $\sigma$-allyl fragment and the computed free-energy barrier too high large, 86 kcal·mol$^{-1}$. Alternatively, the $H_2$ molecule could be primarily added across the Ti-N bond, as it has been computationally proposed for the hydrogenation of dinitrogen by di- and tetra-titanium species.[30,31] Similarly, we have shown that analogous polynuclear titanium complexes were able to activate strong bonds (N-H, C=O, or C-H) via addition across bridging Ti-X bonds (X = N, C).[28a,32a-c] Also, the C-H and N-H bonds can be activated by terminal imido-titanium complexes and their mechanism have been analyzed computationally.[32d,e] Thus, we propose that the reaction starts with the activation of $H_2$ molecule by the $\mu$-imido group in complex **3** leading to an $\mu$-amido hydride complex. The reaction takes place through transition state **TS1** with a free-energy barrier of 33.7 kcal·mol$^{-1}$ to give the intermediate **I1**, which is 19.7 kcal·mol$^{-1}$ above reactants. In intermediate **I1** the Ti-N bond elongates significantly at the Ti-hydride side, from 1.92 Å in **2** to 2.36 Å. We have also evaluated the addition of $H_2$ across the Ti-O bond (see Supporting information Scheme S1) but the computed free-energy barrier is significantly higher, 41.8 kcal·mol$^{-1}$, and the resulting intermediate lays 37.4 kcal·mol$^{-1}$ above reactants. Thus, we can rule out the participation of the $\mu$-oxo moiety in the $H_2$ activation.

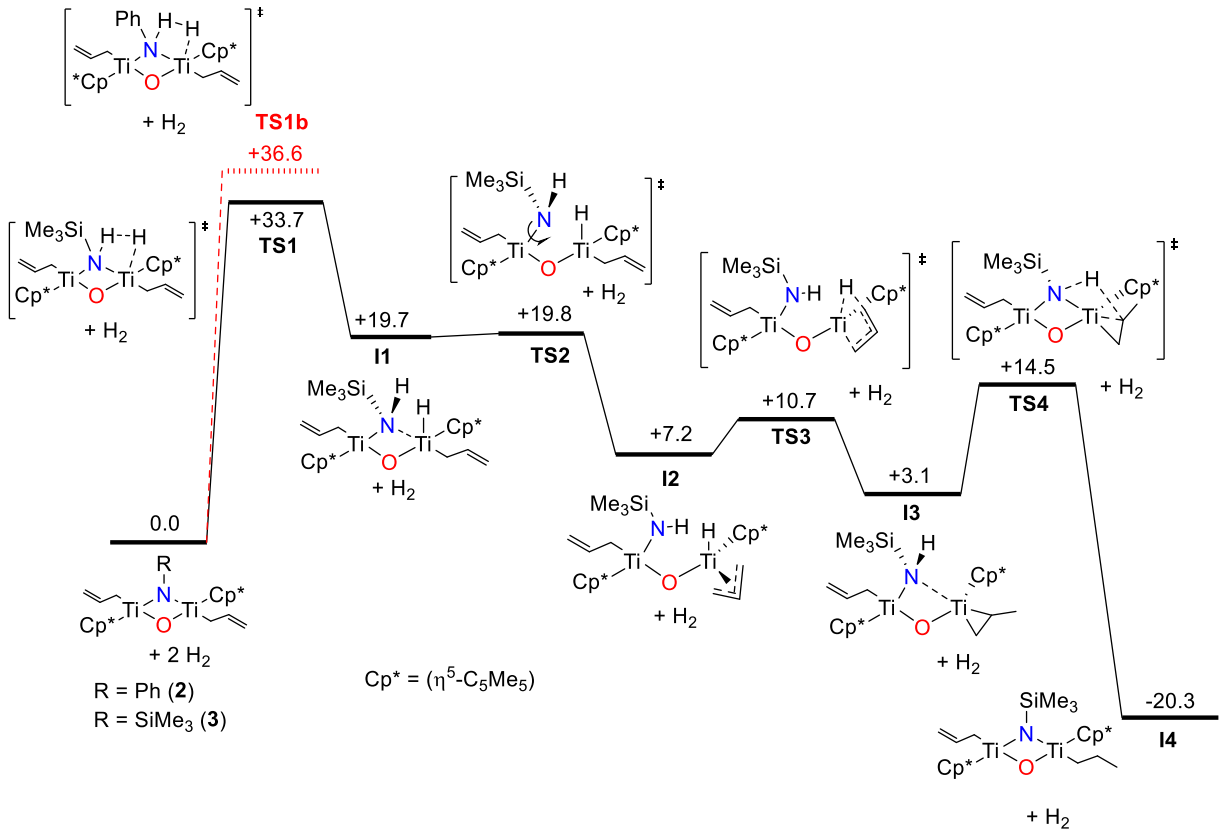


**Figure 8**. Gibbs free energy profile (kcal·mol$^{-1}$) for the hydrogenation process of an allyl fragment in complex **3** (R = $SiMe_3$, solid black line) and comparison of the initial step for complex **2** (R = Ph, dashed red line).

Complex **I1** evolves very rapidly to intermediate **I2** via rearrangement of the amido moiety to form a terminal Ti-amido group (see Figure 8). The process involves also a rearrangement of the distorted trigonal bipyramidal titanium environment in **I1** to a three-legged piano stool environment in **I2**. The transformation of **I1** to **I2** is exergonic by 12.5 kcal·mol$^{-1}$ and its free energy barrier is very low by 0.1 kcal·mol$^{-1}$. This reaction step involves some additional, important structural changes (see Figure 9): i) the NH moiety of amido group forms a hydrogen bond with the Ti-hydride group (H··H distance is 1.810 Å);[33] ii) the allyl fragment changes its hapticity from $\eta^1$ to $\eta^3$, which occurred spontaneously during the optimization process. Both structural features have important implications on the reactivity of step.

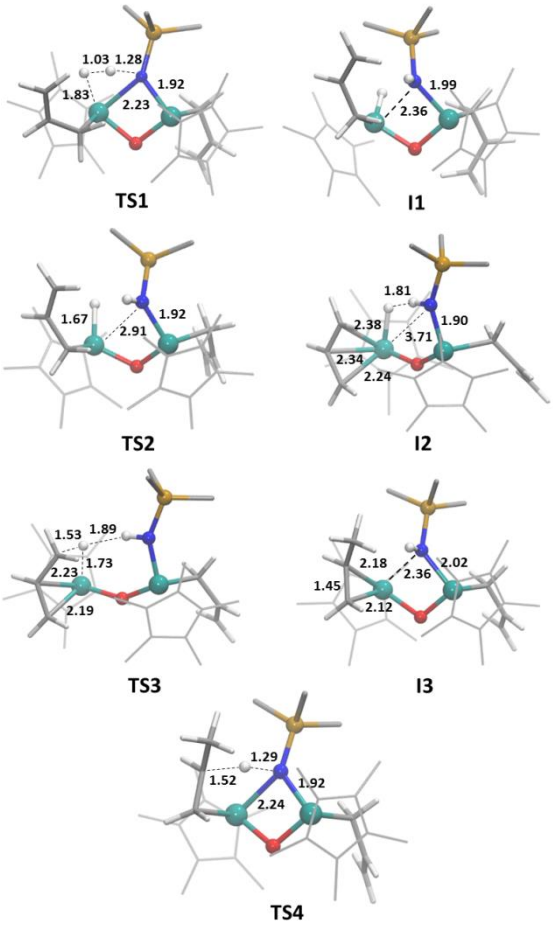


**Figure 9**. DFT computed structures of the intermediates and transition states involved in the reaction mechanism of the hydrogenation of the allyl moiety of complex **3**. Distances in Å.

In **I2** the allyl ligand can insert into the Ti-H bond to give intermediate **I3**.[34] The computed free energy barrier is very low (3.5 kcal·mol$^{-1}$) in part because hydride transfer is assisted by hydrogen bonding from the amide group, as observed in the corresponding transition state **TS3** (Figure 9). This step is exergonic by 4.1 kcal·mol$^{-1}$. In the resulting intermediate **I3**, the titanium formally remains Ti(IV) resulting in a metallacyclopropane complex with the amido group bridging the two titanium centers. The formation of the metallacyclopropane moiety is confirmed by the long C-C bond distance, 1.45 Å, which is closer to the C-C single bond, 1.48 Å, than to the C-C double bond, 1.34 Å, in the $\sigma$-allyl ligand. Moreover, the two interacting carbon atoms deviate significantly from planar $sp^2$ hybridization showing out-of-plane angles of 36º and 41º respectively. These geometric features are similar to those characterized in previous theoretical studies on titanacyclopropane complexes,[35a,b] and other transition metals.[35c]

The final step to complete the hydrogenation consists of the proton abstraction from the amido group by the $\beta$-carbon of the metallacyclopropane complex moiety that has a larger nucleophilic character. The process takes place via transition state **TS4**, which is only 11.4 kcal·mol$^{-1}$ above intermediate **I3**. The partially hydrogenated product **I4** yields one propyl moiety and recovers the original bridging $\mu$-imido group, which can activate a second $H_2$ molecule to hydrogenate the other Ti-$\sigma$-allyl fragment. The whole transformation of **3** to **I4** is exergonic by 20.3 kcal·mol$^{-1}$ and its rate-determining step corresponds to the initial addition of the $H_2$ across the Ti-N bond. The proposed rate-determining step is fully consistent with the fact that the reaction time reduces upon increasing $H_2$ pressure. Importantly, the Ti-$\mu$-imido moiety of complex **3** plays a key role in the activation of $H_2$ to hydrogenate the double bonds.

Finally, in order to elucidate why there is no reaction with complex **2** (R = Ph) at p < 1 atm, we compute the $H_2$ activation step on complex **2** (**TS1b**). The geometrical parameters of **TS1b** are quite similar than those on **TS1** but the free energy barrier is 2.9 kcal·mol$^{-1}$ higher, what can explain the need to increase the $H_2$ pressure (p ≈ 1.5 atm) to observe the reaction in complex **2**. Replacing the trimethylsilyl substituent of the amido group in **3** by the electron-withdrawing phenyl substituent in **2** decreases the polarity of the titanium-imido bond reducing its ability to activate heterolyticallly $H_2$ molecule, as Cundari *et al.*[32d] and Sakaki *et al.*[32e] showed previously in the activation of C-H bonds by titanium-imido complexes. Accordingly, the comparison of charge distribution in complexes **2** and **3** shows that the Ti-N bond in **3** is more polarized and the nitrogen supports a larger negative charge than in **2** (q(N) = -1.07 vs. -0.64 a.u., q(Ti) = +0.85 and +0.84 a.u. for **3** and **2** respectively). Consequently, the titanium-imido moiety of complex **3** is more reactive towards the incoming substrate.

## CONCLUSIONS

We have synthesized and characterized a dinuclear $\mu$-oxo titanium(III) complex comprising two bridging allyl ligands. The analysis of the electronic structure of this species by DFT methods confirm its closed-shell nature and reveals a metal-metal single bond between the two Ti(III) centers. This compound reacts promptly and quantitatively with organic azides ($RN_3$, R = Ph, $SiMe_3$) to afford the corresponding dinuclear $\mu$-imido $\mu$-oxo complexes in which the allyl ligands show different metal-allyl

bonding situations in solution and in the solid state. Furthermore, the treatment of the $\mu$-imido complexes with hydrogen proceeds with hydrogenation of the allyl fragments. The theoretical study characterizes the reaction mechanism for the observed process. It consists of three main steps: i) addition of the $H_2$ across the Ti-N bond to form a dinuclear hydride amido complex, ii) hydride migration to the $\pi$-allyl ligand yielding a metallacyclopropane complex, and iii) final proton transfer from the amido group to lead the propyl complex. Overall, the $\mu$-imido moiety is able to activate the $H_2$ molecules in the presence of substituents that enhance its nucleophilic character. Further studies on the reactivity of the bridging bis-allyl titanium(III) complex toward hydrogen as well as other small molecules are ongoing in our group.

## ASSOCIATED CONTENT

### Supporting Information

The Supporting Information is available free of charge on the ACS Publications website.

Table of crystallographic data for **1**, **2** and **5** (Table S1).

NMR spectra for complexes **1**-**4** (Figures S1-S16).

Different mechanisms analysis of the hydrogenation process (Scheme S1).

Geometrical features of the stationary points and transition states (Figure S17).

Alternative mechanism involving reductive elimination (Figure S18).

Cartesian coordinates in a format for convenient visualization (XYZ).

**Accession Codes**

CCDC 1915051-1915053 contain the supplementary crystallographic data for this paper. These data can be obtained free of charge via www.ccdc.cam.ac.uk/data_request/cif, or by emailing data_request@ccdc.cam.ac.uk, or by contacting The Cambridge Crystallographic Data Centre, 12 Union Road, Cambridge CB2 1EZ, UK; fax: +44 1223 336033.

## AUTHOR INFORMATION


### Corresponding Author

*E-mail: j.carbo@urv.cat (J.J.C.)

*E-mail: cristina.santamaria@uah.es (C.S.)


Notes

The authors declare no competing financial interest.

## ACKNOWLEDGMENT


Financial support for this work was provided by the Ministerio de Ciencia, Innovación y Universidades (PGC2018-094007-B-I00), the Universidad de Alcalá (CCG2018/EXP-026) and the Generalitat de Catalunya (2014SGR199).


## REFERENCES


(1) Smidt, J.; Hafner, W. Eine Reaktion von Palladiumchlorid mit Allylalkohol. *Angew. Chem*. **1959**, *71*, 284.

(2) For a comprehensive review on metal allyl complexes: a) Green, M. L. H.; Nagy, P. L. I. Allyl metal complexes. *Adv. Organomet. Chem*. **1965**, *2*, 325-363. b) Powell, P. Synthesis of $\eta^3$-allyl complexes. In The chemistry of the metal-carbon bond; Hartley, F. R., Patai S. Eds.; John Wiley & Sons, 1982; Vol. 1, pp 325-366.

(3) For a selection, see: a) Evans, W. J.; Ulibarri, T. A.; Ziller, J. W. Reactivity of $(C_5Me_5)$Sm and Related Species with Alkenes: Synthesis and Structural Characterization of a Series of Organosamarium Allyl Complexes. *J. Am. Chem. Soc*. **1990**, *112*, 2314-2324. b) Evans, W. J.; Kozimor, S. A.; Brady, J. C.; Davis, B. L.; Nyce, G. W.; Seibel, C. A.; Ziller, J. W.; Doedens, R. J. Metallocene Allyl Reactivity in the Presence of Alkenes Tethered to Cyclopentadienyl Ligands *Organometallics* **2005**, *24*, 2269-2278. c) Webster, C. L.; Ziller, J. W.; Evans. W. J. Synthesis and $CO_2$ Insertion Reactivity of Allyluranium Metallocene Complexes. *Organometallics* **2012**, *31*, 7191-7197.

(4) a) Nakamoto, K. Infrared and Raman Spectra of Inorganic and Coordination Compounds, Part B: Applications in Coordination, Organometallic, and Bioinorganic Chemistry, 6th Ed, John Wiley and Sons, Inc., New Jersey, 2009. b) Lichtenberg, C.; Okuda. J. Structurally Defined Allyl Compounds of Main Group Metals: Coordination and Reactivity. *Angew. Chem. Int. Ed.* **2013**, *52*, 5228-5246.

(5) For a selection, see: a) Marion, N.; Navarro, O.; Mei, J.; Stevens, E. D.; Scott, N. M.; Nolan. S. P. Modified (NHC)Pd(allyl)Cl (NHC = N-Heterocyclic Carbene) complexes for room-temperature Suzuki-Miyaura and Buchwald-Hartwig reactions. *J. Am. Chem. Soc.* **2006**, *128*, 4101-4111. b) Markert, C.; Neuburger, M.; Kulicke, K.; Meuwly, M.; Pfaltz A. Palladium-catalyzed allylic substitution: reversible formation of allyl-bridged dinuclear palladium(I) Complexes. *Angew. Chem. Int. Ed*. **2007**, *46*, 5892-5895. c) Hruszkewycz, D. P.; Wu, J.; Hazari,

N.; Incarvito, C. D. Palladium(I)-bridging allyl dimers for the catalytic functionalization of $CO_2$. *J. Am. Chem. Soc.* **2011**, *133*, 3280-3283. d) Hazari, N.; Hruszkewycz, D. P.; Wu, J. Pd(I)-bridging allyl dimers: a new system for the catalytic functionalization of carbon dioxide. *Synlett.* **2011**, *13*, 1793–1797.

(6) a) Chisholm, M. H.; Hampden-Smith, M. J.; Huffman J. C. Diallyl- and bis(2-methylallyl)tetrakis(dimethylamido)ditungsten: $W_2(\mu\text{-}\eta^3\text{-}C_3H_5)_2(NMe_2)_4$ and $W_2(\eta^1\text{-}C_4H_7)_2(NMe_2)_4$ (M≡M). Comments on ligand-metal $\pi$-interactions at $(M{\equiv}M)^{6+}$ Centers. *J. Am. Chem. Soc.* **1988**, *110*, 4070-4071. b) Song, L. C.; Cheng, J.; Gong, F. H.; Hu, Q. M.; Yan, J. Synthesis and characterization of starlike complexes containing three terminal butterfly Fe/S cluster cores generated via reactions of the three-$\mu$-CO-containing trianions $\{[(\mu\text{-}CO)Fe_2(CO)_6]_3[(\mu\text{-}SCH_2CH_2)_3N]\}^{3-}$ and $\{[(\mu\text{-}CO)Fe_2(CO)_6]_3[1,3,5\text{-}(\mu\text{-}SCH_2)_3C_6H_3]\}^{3-}$ with electrophiles. *Organometallics* **2005**, *24*, 3764-3771. c) Trovitch, R. J.; John, K. D.; Martin, R. L.; Obrey, S. J.; Scott, B. L.; Sattelberger, A. P.; Baker, R. T. Interplay of metal–allyl and metal–metal bonding in dimolybdenum allyl complexes. *Chem. Commun.* **2009**, 4206-4208. d) Riener, K.; Zimmermann, T. K.; Pöthig, A.; Herrmann, W. A.; Kühn F. E. Direct synthesis and bonding properties of the first $\mu\text{-}\eta^2,\eta^2$-allyl-bridged diiridium complex. *Inorg. Chem.* **2015**, *54*, 4600−4602.

(7) Cotton, F. A.; Murillo, C. A.; Petruknina, M. A. Novel $\eta^3$-allyl complexes of titanium. *J. Organomet. Chem.*, **2000**, *593-594*, 1-6.

(8) Palacios, F.; Royo, P.; Serrano, R.; Balcazar, J. L.; Fonseca, I.; Florencio, F. The hydrolisis of pentamethylcyclopentadienyltitanium trihalides and the formation of di-, tri- and tetra-nuclear $\mu$-oxo complexes. Crystal structure of $[(C_5Me_5)TiBr(\mu\text{-}O)]_4{\cdot}CHCl_3$, which contains a $Ti_4O_4$ ring. *J. Organomet. Chem*. **1989**, *375*, 51-58.

(9) Farrugia, L. J. WinGX and ORTEP for Windows: an update. *J. Appl. Crystallogr*. **2012**, *45*, 849−854.

(10) a) Sheldrick, G. M. Crystal structure refinement with SHELXL. Acta Crystallogr. 2015, C71, 3−8. b) Sheldrick, G. M. A short history of SHELX. *Acta Crystallogr., Sect. A: Found. Crystallogr*. **2008**, *64*, 112−122.

(11) Frisch, M. J.; Trucks, G. W.; Schlegel, H. B.; Scuseria, G. E.; Robb, M. A.; Cheeseman, J. R.; Scalmani, G.; Barone, V.; Petersson, G. A.; Nakatsuji, H.; Li, X.; Caricato, M.; Marenich, A. V.; Bloino, J.; Janesko, B. G.; Gomperts, R.; Mennucci, B.; Hratchian, H. P.; Ortiz, J. V.; Izmaylov, A. F.; Sonnenberg, J. L.; Williams-Young, D.; Ding, F.; Lipparini, F.; Egidi, F.; Goings, J.; Peng, B.; Petrone, A.; Henderson, T.; Ranasinghe, D.; Zakrzewski, V. G.; Gao, J.; Rega, N.; Zheng, G.; Liang, W.; Hada, M.; Ehara, M.; Toyota, K.; Fukuda, R.; Hasegawa, J.; Ishida, M.; Nakajima, T.; Honda, Y.; Kitao, O.; Nakai, H.; Vreven, T.; Throssell, K.; Montgomery, J. A., Jr.; Peralta, J. E.; Ogliaro, F.; Bearpark, M. J.; Heyd, J. J.; Brothers, E. N.; Kudin, K. N.; Staroverov, V. N.; Keith, T. A.; Kobayashi, R.; Nor-mand, J.; Raghavachari, K.; Rendell, A. P.; Burant, J. C.; Iyengar, S. S.; Tomasi, J.; Cossi, M.; Millam, J. M.; Klene, M.; Adamo, C.; Cammi, R.; Ochterski, J. W.; Martin, R. L.; Morokuma, K.; Farkas, O.; Foresman, J. B.; Fox, D. J. Gaussian 16, Revision A.03; Gaussi-an, Inc., Wallingford CT, 2016.

(12) Parr, R. G.; Yang, W. Density Functional Theory of Atoms and Molecules; Oxford University Press:Oxford, U.K., 1989.

(13) a) Lee, C.; Yang, W.; Parr, R. G. Development of the Colle-Salvetti correlation-energy formula into a functional of the electron density. Phys. Rev. B: *Condens. Matter Mater. Phys*. **1988**, *37*, 785-789. b) Becke, A. D. Density-functional thermochemistry. III. The role of exact exchange. *J. Chem. Phys.* **1993**, *98*, 5648-5652. c) Stephens, P. J.; Devlin, F. J.; Chabolowski, C. F.; Frisch, M. J. Ab Initio Calculation of Vibrational Absorption and Circular Dichroism Spectra Using Density Functional Force Fields. *J. Phys. Chem*. **1994**, *98*, 11623-11627.

(14) Hay, P. J; Wadt, W. R. Ab initio effective core potentials for molecular calculations. Potentials for K to Au including the outermost core orbitals. *J. Chem. Phys.* **1985**, *82*, 299-310.

(15) a) Höllwarth, A.; Böhme, M.; Dapprich, S.; Ehlers, A. W.; Gobbi, A.; Jonas, V.; Köler, K. F.; Stegmann, R.; Veldkamp, A.; Frenking, G. A set of d-polarization functions for pseudo-potential basis sets of the main group elements Al-Bi and f-type polarization functions for Zn, Cd, Hg. *Chem. Phys. Lett.* **1993**, *208*, 237-240. b) Ehlers, A. W.; Böhme, M.; Dapprich, S.; Gobbi, A.; Höllwarth, A.; Jonas, V.; Köhler, K. F.; Stegmann, R.; Veldkamp, A.; Frenking, G. A set of f-polarization functions for pseudo-potential basis sets of the transition metals Sc-Cu, Y-Ag and La-Au. *Chem. Phys. Lett.* **1993**, *208*, 111-114.

(16) a) Francl, M. M.; Pietro, W. J.; Hehre, W. J.; Binkley, J. S.; Gordon, M. S.; DeFrees, D. J.; Pople, J. A. Self−consistent molecular orbital methods. XXIII. A polarization-type basis set for second-row elements. *J. Chem. Phys.* **1982**, *77*, 3654-3665. b) Hehre, W. J.; Ditchfield, R.; Pople, J. A. Self—Consistent Molecular Orbital Methods. XII. Further Extensions of Gaussian—Type Basis Sets for Use in Molecular Orbital Studies of Organic Molecules. *J. Chem. Phys.* **1972**, *56*, 2257-2261. c) Hariharan, P. C.; Pople, J. A. The influence of polarization functions on molecular orbital hydrogenation energies. *Theor. Chim. Acta* **1973**, *28*, 213-222.

(17) Grimme, S.; Antony, J.; Ehrlich, S.; Krieg, H. A consistent and accurate ab initio parametrization of density functional dispersion correction (DFT-D) for the 94 elements H-Pu. *J. Chem. Phys.* **2010**, *132*, 154104.

(18) Reed, R.; Curtiss, L. A.; Weinhold, F. Intermolecular interactions from a natural bond orbital, donor-acceptor viewpoint. *Chem. Rev*. **1988**, *88*, 899–926.

(19) Gonzalez-Pérez, J. I.; Martín, A.; Mena, M.; Santamaría. C. C-H activation on an oxo-bridged dititanium complex: From alkyl to $\mu$-alkylidene functionalities. *Organometallics* **2016**, *35*, 2488-2493.

(20) Chen, J.; Kai, Y.; Kasai, N.; Yasuda, H.; Yamamoto, H.; Nakamura, A. Steric effect of allyl substituent on the molecular structures of allyltitanium complexes. *J. Organomet. Chem*., **1991**, *407*, 191-205.

(21) Cayton, R. H.; Chisholm, M. H.; Hampden-Smith, M. J.; Huffman, J. C.; Moodley, K. G. The tungsten-tungsten triple bond-18. Bridging and terminal allyl ligands in complexes of the formula $W_2(R)_2(NMe_2)_4$, where R = $C_3H_5$ and $C_4H_7$. *Polyhedron*, **1992**, *24*, 3197-3210.

(22) a) S. García Blanco, M. P. Gómez Sal, S. Martínez Carreras, M. Mena, P. Royo, R. Serrano. Hydrolytic studies on ($\eta^5$-$C_5Me_5$)$TiMe_3$; X-ray structure of [($\eta^5$-$C_5Me_5$)$TiMe(\mu$-O)]$_3$ containing a $Ti_3O_3$ ring. *J. Chem. Soc., Chem. Commun*. **1986**, 1572-1573. b) Gómez-Sal P.; Martín, M.; Mena, M.; Yélamos, C. Synthesis of the Organotitanoxane Complexes [($\eta^5$-$C_5Me_5)_4Ti_4X_2$]($\mu$-O)$_5$. X-ray Structure of [($\eta^5$-$C_5Me_5)_4Ti_4Me_2$]($\mu$-O)$_5$. *Inorg. Chem.* **1996**, *35*, 242-243.

(23) Gómez-Sal, P.; Mena, M.; Palacios, F.; Royo, P.; Serrano, R.; Martínez-Carreras, S. Preparation of the compounds ($\mu$-O)[Ti($C_5Me_5$)$R_2$]$_2$ (R = Me, $CH_2Ph$, or $CH_2SiMe_3$) and the crystal structure of the derivative with R = $CH_2SiMe_3$. *J. Organomet. Chem.* **1989**, *375*, 51-58.

(24) a) Metal-Metal Multiple Bonds. 22. Addition Reactions of Organic Azides and Diethyl Azodicarboxylate with $Cp_2Mo_2(CO)_4$. Molecular Structures of $Cp_2Mo_2(CO)_2(NAr)(\mu$-NNN(Ar)CO) (Ar = p-t-$BuC_6H_4$) and [Cp'Mo$(CO)_2]_2(\mu$-$EtO_2CN_2CO_2Et$). *Organometallics* **1987**, *6*, 2151-2157. b) Proulx, G.; Bergman, R. G. Synthesis, Structures, and Kinetics and Mechanism of Decomposition of Terminal Metal Azide Complexes: Isolated Intermediates in the Formation of Imidometal Complexes from Organic Azides. *Organometallics* **1996**, *15*, 684-692.

(25) Gómez-Sal, P., Martín, A., Mena, M., Morales, M. C., Santamaría, C. Photochemical incorporation of N-benzylidene(phenyl) amine into the complex [{Ti($\eta^5$-$C_5Me_5$)($\mu$-O)}$_3$($\mu_3$-CH)] as a model of the titanium oxide surface. *Chem. Commun*., **1999**, 1839-1840.

(26) Nagae, H.; Hato, W.; Kawakita, K.; Tsurugi, H.; Mashima K. Arylimido-bridged Dinuclear Ti($\mu$-NAr)$_2$Ti Scaffold for Alkyne Insertion into the Ortho-C-H Bond of Arylimido Ligands. *Chem. Eur. J.* **2017**, *23*, 586-596.

(27) Vidal, F., Davila, M. A., Torcuato, A. S., Gómez-Sal, P., Mosquera, M. E. G. Functionalized Imido-bridged Ti(IV) Complexes as New Building Blocks for Supramolecular Arrangements: Generation of a 1D Structure through a Mg–Cl···I–C Halogen Bonding Interaction. *Dalton Trans.*, **2013**, *42*, 7074-7084.

(28) For some examples of dinuclear titanium $\mu$-oxo complexes, see: a) Carbó, J. J., García-López, D.; Gómez-Pantoja, M.; González-Pérez, J. I.; Martín, A.; Mena, M.; Santamaría, C. Intermetallic Cooperation in C−H Activation Involving Transient Titanium-Alkylidene Species: A Synthetic and Mechanistic Study. *Organometallics* **2017**, *36*, 3076−3083. b) Gómez-Pantoja, M.; González-Pérez, J. I.; Martín, A.; Mena, M.; Santamaría, C.; Temprado, M. Reactivity of Tuck-over Titanium Oxo Complexes with Isocyanides. *Organometallics* **2018**, *37*, 2046−2053.

(29) Gómez, M.; González-Pérez, J. I.; Hernández-Prieto, C.; Martín, A.; Mena, M.; Santamaría, C. Molecular Design of Cyclopentadienyl Tantalum Sulfide Complexes. *Inorg. Chem*. **2019**, *58*, 5593-5602.

(30) Martinez, S.; Morokuma, K.; Musaev, D. G. Mechanistic Aspects of Dinitrogen Hydrogenation Catalyzed by the Geometry-Constrained Zirconium and Titanium Complexes: Computational Studies. *Organometallics* **2007**, *26*, 5978-5986.

(31) a) Wang, B.; Luo, G.; Nishiura, M.; Hu, S.; Takanori, S.; Luo, Y.; Hou, Z. Dinitrogen Activation by Dihydrogen and a PNP-Ligated Titanium Complex. *J. Am. Chem. Soc.* **2017**, 139, 1818-1821. b) Takanori, S.; Luo, G.; Hu, S.; Luo, Y.; Hou, Z. Experimental and Computational Studies of Dinitrogen Activation and Hydrogenation at a Tetranuclear Titanium Imide/Hydride Framework. *J. Am. Chem. Soc*. **2019**, *141*, 2713-2720.

(32) a) Carbó, J. J.; Martín, A.; Mena, M.; Pérez-Redondo, A.; Poblet, J. M.; Yélamos, C., Addition of Terminal Alkynes to a Molecular Titanium–Zinc Nitride. *Angew. Chem. Int. Ed.* **2007**, *46*, 3095 –3098 b) Aguado-Ullate, S.; Carbó, J. J.; González-del Moral, O.; Martín, A.; Mena, M.; Poblet, J. M.; Santamaría, C. Ammonia Activation by $\mu_3$-Alkylidyne Fragments Supported on a Titanium Molecular Oxide Model. *Inorg. Chem.* **2011**, *50*, 6269–6279; c) Carbó, J. J., García-López, D.; González-del Moral, O.; Martín, A.; Mena, M.; Santamaría, C., Carbon−Nitrogen Bond Construction and Carbon−Oxygen Double Bond Cleavage on a Molecular Titanium Oxonitride: A Combined Experimental and Computational Study. *Inorg. Chem*. **2015**, *54*, 9401−9412. d) Cundari, T. R.; Klinckman, T. R.; Wolczanski, P. T., Carbon-Hydrogen Bond by Titanium Imido Complexes. Computational Evidence for the Role of Alkene Adducts in Selective C-H Activation. *J. Am. Chem. Soc.* **2002**, *124*, 1481-1487. e) Ochi, N.; Nakao, Y.; Sato, H.; Sakaki, S., Theoretical study of C-H and N-H Sigma-Bond Activation Reactions by Titanium(IV)-Imido Complex. Good Understanding Based on Orbital Interaction and Theoretical Proposal for N-H Sigma-Bond Activation of Ammonia. *J. Am. Chem. Soc.* **2007**, *129*, 8615-8624.

(33) a) Lee, J. C.; Peris, Jr. E.; Rheingold, A. L.; Crabtree, R. H. An Unusual Type of H···H Interaction: Ir-H···H-O and Ir-H···H-N Hydrogen Bonding and Its Involvement in σ-Bond Metathesis. *J. Am. Chem. Soc*. **1994**, *116*, 11014-11019. b) Shubina, E. S.; Belkova, N. V.; Krylov. A. N.; Vorontsov E.V.; Epstein, L. M.; Gusev, D. G.; Niedermann, M.; Berke, H. Spectroscopic Evidence for Intermolecular M-H···H-OR Hydrogen Bonding: Interaction of WH(CO)$_2$(NO)L$_2$ Hydrides with Acidic Alcohols. *J. Am. Chem. Soc*. **1996**, *118*, 1105-1112.

(34) a) Bochmann, M. Organometallics 2. Complexes with Transition Metal-Carbon $\pi$-Bonds. Oxford University Press Inc., New York, 1994, p 66. b) Hartwig, J. F. Organotransition Metal Chemistry: From Bonding to Catalysis. University Science Books: Sausalito, 2009. c) Ryan, D. E.; Cardin, D. J.; Hartl, F. $\eta^3$-Allyl carbonyl complexes of group 6 metals: Structural aspects, isomerism, dynamic behavior and reactivity. *Coord. Chem. Rev*. **2017**, *335*, 103-149. and references herein.

(35) a) Steigerwald, M. L.; Goddard III, W. A. Dichlorotitanacyclopropane. The Structure and Reactivity of a Metallacyclopropane. *J. Am. Chem. Soc.* **1985**, *107*, 5027-5035. b) Cho, H.; Andrews, L. C-H Activation of Ethane by Group 4 Metal Atoms: Observation and Characterization of the $MH\text{-}CH_2CH_3$, $MH_2\text{-}(CH_2)_2$, and $MH_3\text{-}CH{=}CH_2$ Complexes. *J. Phys. Chem. A* **2008**, *112*, 1519-1525. c) Carbó, J. J.; Crochet, P.; Esteruelas, M. A.; Jean, Y.; Lledós, A.; López, A. M.; Oñate, E. Two- and Four-Electron Alkyne Ligands in Osmium-Cyclopentadienyl Chemistry: Consequences of the $\pi_\perp \rightarrow M$ Interaction. *Organometallics* **2002**, *21*, 305-314.

## Table of Contents Graphic

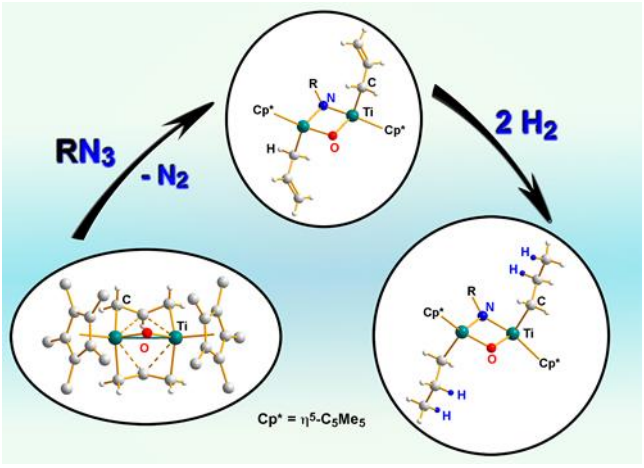


## Table of Contents Synopsis

A diamagnetic dinuclear bridging allyltitanium(III) derivative was synthesized, and DFT calculations on its electronic structure and nature of bonding were performed. The reactivity of this species towards organic azides has rendered a series of dimetallic $\mu$-imido $\mu$-oxo allyl complexes. Related to the latter, the hydrogenation processes of the allyl fragments were discussed both experimentally and theoretically.